Nanoscale Advances

ROYAL SOCIETY OF CHEMISTRY

PAPER

View Article Online
View Journal

Cite this: DOI: 10.1039/d5na00419e

Dexamethasone-loaded lipid-polymeric nanoparticles to improve therapy for cisplatin-induced sensorineural hearing loss

Wang Qi, † Huang Qiling,† Li Liling,† Li Zhicheng, Li Peng* and Zeng Xiangli*

Sensorineural hearing loss (SNHL), caused by ototoxic drugs like cisplatin, poses significant challenges due to its irreversible nature. Dexamethasone, a potent corticosteroid, is commonly used to mitigate SNHL but suffers from systemic side effects and poor inner ear bioavailability when administered conventionally. This study explores the potential of dexamethasone-loaded lipid-polymeric nanoparticles (LPNs) to enhance drug delivery efficiency and therapeutic outcomes. The LPNs were fabricated using stearic acid and poly (lactic-*co*-glycolic acid) (PLGA) *via* a double emulsion solvent evaporation method, combining the biocompatibility of lipid nanoparticles with the sustained-release properties of polymeric nanoparticles. Characterization revealed optimal particle size (~150 nm by SEM and ~380 nm by LDE), polydispersity index (PDI 0.233), and ζ-potential (−21.9 mV), ensuring colloidal stability and cellular uptake. *In vitro* studies demonstrated sustained dexamethasone release over 72 hours, with 55.56% released within 4 hours. HEI-OC1 cell viability assays confirmed the LPNs' cytocompatibility and superior protection against cisplatin-induced cytotoxicity compared to raw dexamethasone. *In vivo* experiments in a cisplatin-induced ototoxicity mouse model showed enhanced cochlear drug distribution, peaking at 24 hours, and significantly reduced auditory brainstem response (ABR) thresholds at 16 kHz and 32 kHz post-intratympanic injection. These findings highlight the LPNs' potential as a targeted, sustained-release delivery system for treating SNHL, offering improved efficacy and reduced systemic exposure. This study provides a foundation for clinical translation of LPN-based therapies in otoprotection.

Received 30th April 2025
Accepted 15th October 2025

DOI: 10.1039/d5na00419e

rsc.li/nanoscale-advances

1. Introduction

Sensorineural hearing loss (SNHL) is a prevalent and often irreversible condition that impacts millions of people, affecting their quality of life. SNHL arises from damage to the hair cells of the cochlea or the auditory nerve, leading to a decline in the ability to perceive sound. Cisplatin, a widely used chemotherapeutic agent, is known to cause ototoxicity and SNHL. Cisplatin induces bilateral, permanent sensorineural hearing loss in a staggering 80% of cancer patients, with many also experiencing the distressing symptom of tinnitus.[1] Approximately 500 000 new patients each year were recorded[2,3] and dexamethasone is a standard treatment with proven protective effects against cisplatin-induced ototoxicity.[4] Dexamethasone is a potent corticosteroid with anti-inflammatory and immunosuppressive properties.[5,6] It has been widely recognized for its potential to mitigate inflammation and protect auditory cells, making it the most common medication prescribed for SNHL treatment.[7]

Systemic dexamethasone, despite its therapeutic benefits, can lead to adverse effects such as acneiform eruptions, desquamation of the skin, osteoporosis or osteonecrosis, opportunistic infections, and suppression of the adrenal cortex. These adverse effects arise due to its high affinity for glucocorticoid receptors.[8–10] Intratympanic injection is an alternative method to avoid systemic side effects associated with dexamethasone.[11] However, the eustachian tube allows a substantial amount of the medication to escape, which poses a significant challenge. Additionally, the intricate structure of the inner ear and the presence of the round window membrane further complicate drug penetration to the cochlea.[12,13] Beyond that, dexamethasone's water insolubility feature also impacts its bioavailability in the inner ear. These factors impede the drug from achieving therapeutic concentrations in the target area, thereby diminishing its protective impact and overall effectiveness in the treatment of SNHL.

To address this challenge, researchers have been exploring innovative drug delivery systems that can enhance the bioavailability and targeted delivery of dexamethasone to the inner ear. However, current approaches exhibit significant limitations that warrant further investigation. Creber *et al.* utilized a hyaluronic acid sponge combined with histamine to

Department of Otorhinolaryngology-Head and Neck Surgery, The Third Affiliated Hospital of Sun Yat-sen University, 600 Tianhe Road, Tianhe District, 510000 Guangzhou, Guangdong, China. E-mail: zxiangl@mail.sysu.edu.cn; lipeng25@mail.sysu.edu.cn

† These authors contributed equally to this work.

increase the dexamethasone concentration in the inner ear, yet the additional histamine may potentially exacerbate inner ear damage.[14] Kim *et al.* developed poly (lactic-*co*-glycolic acid) nanoparticles within thermosensitive gels to control drug release from the middle ear, but this method may intensify the ear-plugging effect experienced by patients.[15] Furthermore, while biodegradable round window disks[16] have been developed to achieve sustained local drug delivery to the inner ear, they require additional surgical procedures and carry potential risks of inner ear damage. Consequently, there remains a pressing need to develop delivery systems that are not only simple and convenient but also designed for rapid absorption.

Lipid-polymeric nanoparticles (LPNs) represent a significant advancement in this field. These integrated systems combine the biomimetic properties of lipids with the structural advantages of a polymer core, theoretically creating a superior delivery platform. LPNs possess the unique capability to encapsulate drugs, protect them from degradation, and facilitate their transport across biological barriers, thereby enhancing the efficiency of drug delivery to the inner ear.[17,18] The potential of LPNs has been demonstrated in various applications, including their use as vaccine delivery systems to control antigen release and co-deliver immunostimulatory molecules.[19] Additionally, LPNs are being developed for tumor-selective delivery of anticancer agents, enhancing cell-kill efficacy while protecting healthy tissues from cytotoxic exposure, thereby reducing systemic toxicity.[20,21] These advantageous properties can be effectively extended to inner ear drug delivery systems. Notably, there is currently no research focusing on stearic acid-PLGA hybrid nanoparticle delivery systems for inner ear drug administration.

Herein, we aim to investigate the potential of LPNs as a nanocarrier for dexamethasone, focusing on their ability to enhance drug delivery efficiency both *in vitro* and *in vivo*. We will encapsulate dexamethasone within LPNs using stearic acid and PLGA as lipid and polymeric encapsulants respectively. PLGA constitutes the biodegradable and high hydrophobic core which is surrounded by biocompatible stearic acid to facilitate membrane penetration.[22,23] The therapeutic efficacy of this system will be systematically evaluated through a two-phase approach: first using HEI-OC1 cells, an *in vitro* model derived from cochlear outer hair cells that replicates key characteristics of inner ear physiology was established,[24] followed by validation in a well-characterized cisplatin-induced sensorineural hearing loss mouse model.[25] Our study introduced an innovative drug delivery system of intratympanic injection of dexamethasone-loaded LPNs, which reduced systemic exposure from intravenous injection and increased inner ear local bioavailability. These nanocarriers offered a controlled and sustained release of the dexamethasone that can protect auditory cells from cisplatin-induced damage.

2. Materials and methods

2.1 Materials

Stearic acid (HY-B2219), PLGA (HY-B2247A), dexamethasone (HY-14648), polyvinyl alcohol (PVA) (HY-Y0850) and polyethylene glycol 400 (PEG-400) (HY-Y0873A) were purchased from MedChemExpress (USA). Dichloromethane (DCM) (MKL-D821466), paraformaldehyde (PFA) (P885233) and acetonitrile (A960504) were the products of Macklin (China). Coumarin-6 (V900515) and KH_2PO_4(PHR1330) were purchased from Sigma (Germany). Dulbecco's Modified Eagle Medium (DMEM) (C11995500BT) and phosphorus buffer solution (PBS) (C10010500BT) were purchased from ThermoFisher (USA). HEI-OC1 cells were purchased from the Chinese Academy of Sciences (China). FBS (Fetal Bovine Serum) (KF-FBS002) was purchased from Kefan (China). CCK-8 assay (KGA317) was purchased from KeyGEN (China).

2.1.1 Preparation of lipid-polymeric nanoparticles (LPNs). LPNs were prepared by the double emulsion solvent evaporation (DESE) method using stearic acid and PLGA as a matrix and PEG-400 as a stabilizer. The process followed the work of Iqbal *et al.* with some modifications.[26] Briefly, 10 mg stearic acid and PLGA were mixed and dissolved in 2 mL dichloromethane (DCM) as the organic phase, whilst 10 mg dexamethasone was suspended in 0.2 mL deionized (DI) water, making the ratio of the water phase over the organic phase equal to 1 : 10 (v/v). The water phase containing dexamethasone was added to the organic phase containing stearic acid and PLGA, and ultrasonic emulsification was performed for 1 minute (30% amplitude). The emulsified mixture was then quickly poured into 5 mL polyvinyl alcohol (PVA) solution; the PVA solution concentration was 0.5% (w/v), and the same amount of PEG-400 as dexamethasone was dissolved. After pouring the mixture into PVA solution, ultrasonic emulsification was repeated for 1 minute (30% amplitude) to obtain the LPNs loaded with dexamethasone. The obtained LPNs were poured into 15 mL PVA solution of the same concentration. The particles were then magnetically stirred overnight at room temperature to volatilize DCM, then centrifuged to remove the supernatant, and washed with DI water twice. The obtained LPNs would be freeze-dried and stored at −20 °C for subsequent experiments.

Fluorescent LPNs (Coumarin-6-loaded) were prepared using the same DESE protocol as above, except that Coumarin-6 (1% w/w relative to the total polymer and lipid) was co-dissolved with stearic acid and PLGA in the organic phase (DCM). All other compositions and processing parameters (phase ratio, PVA concentration, PEG-400 amount, sonication time/amplitude, and solvent removal/stirring) were identical. The resulting particles were washed twice with DI water, freeze-dried, and stored at −20 °C for subsequent analyses.

2.2 Characterization of dexamethasone-loaded LPNs

2.2.1 Physical characterization of dexamethasone-loaded LPNs. For fabricated LPNs, the particle size, polydispersity index (PDI) and ζ potential were determined at a 2.0 mg ml^{-1} concentration in DI water by using laser Doppler electrophoresis (LDE). Particle size, PDI and ζ – potential are important parameters to evaluate the quality of nanoparticles, which affect their stability, biological distribution and cell uptake.

The morphology of the nanosphere formulations was assessed by Field Emission Scanning Electron Microscopy

(FESEM JEOL JSM-6340F America, Inc.; Pleasanton, CA). Freeze dried dexamethasone-loaded LPNs were placed on a carbon-backed adhesive and sputter-coated with Au for 40 seconds at 20 mA and imaged on a scanning electron microscope with an accelerating voltage of 5 kV. The presence of dexamethasone within the LPNs was confirmed through Fourier Transform Infrared Spectroscopy (FTIR) using a PerkinElmer Frontier. The analysis covered the spectral range of 400 cm^{-1} to 4000 cm^{-1} with a resolution of 1 cm^{-1}, including assessments of native dexamethasone, stearic acid, PLGA, PVA, PEG-400, and the fabricated dexamethasone-loaded LPNs.

2.2.2 *In vitro* release of dexamethasone-loaded LPNs. The drug content in the nanoparticles was quantified by high performance liquid chromatography (HPLC) using a Thermo Scientific Accucore™ C18 column (4.6 × 100 mm, particle size 2.6 μm). Briefly, 10 mg of freeze-dried dexamethasone-loaded LPNs were weighed and dissolved in 5.5 ml acetonitrile with a water bath at 60 °C. Upon full dissolution, 4.5 ml DI water was added and mixed well, followed by centrifugation at 17 000 ×*g* for 5 min to collect the supernatant. The drug content in the supernatant was then determined by using the HPLC method. To prepare the mobile phase for HPLC, acetonitrile and 0.025M KH_2PO_4 buffer (pH 3) were mixed with a volume ratio of acetonitrile to buffer 5.5 : 4.5 (v/v). The mobile phase flow rate was 0.8 ml min^{-1}. The wavelength and temperature were 248 nm and 35 °C, respectively. The retention time is 15 min.

To evaluate the release of dexamethasone from LPNs, an *in vitro* release study under sink conditions was carried out. Briefly, 30 mg dexamethasone-loaded LPNs were weighed and added into 5 ml 1× PBS solution. For the control group, raw dexamethasone with an equivalent amount of drug in 30 mg LPNs was weighed and added into 5 ml 1× PBS solution for comparison. The mixtures were incubated at 37 °C with continuous shaking at 120 rpm for 1 week to ensure uniform distribution and facilitate the release of dexamethasone. At each set time point (1 h, 2 h, 3 h, 4 h, 6 h, 28 h, 48 h, 72 h, and 168 h), the mixtures were forwarded for centrifugation at 17 000 ×*g*. After 30 min of centrifugation, 4 ml supernatant was withdrawn for dexamethasone quantification using HPLC, while 4 ml fresh 1× PBS solution was added afterwards.

2.2.3 Cell proliferation assay. HEI-OC1 cells were seeded into 96-well plates (Corning, USA) at a density of 1 × 10^5 cells per well in DMEM complete culture medium (supplemented with 10% FBS) and allowed to adhere for 24 hours at 37 °C in a humidified incubator (Thermo Fisher Scientific, USA) containing 5% CO_2.[27] Following adhesion, the culture medium was replaced with 100 μL of fresh DMEM complete medium containing either dexamethasone or dexamethasone-loaded LPNs at concentrations of 0.8, 1.6, 3.2, 6.4, 12.8, and 25.6 μg ml^{-1}. Cells were incubated with the treatments for 12, 24, 36, or 48 hours at 37 °C under 5% CO_2. Cell viability was subsequently assessed using the Cell Counting Kit-8 (CCK-8) assay according to the manufacturer's protocol.[28] Briefly, 10 μL of the CCK-8 solution was added directly to each well and the plate was incubated for an additional 2 hours at 37 °C. The absorbance of each well was then measured at 450 nm using a microplate reader (BioTek, USA). Wells containing medium plus CCK-8 without cells served as blanks for background subtraction. Cell viability was calculated relative to untreated control cells.

2.2.4 LPN cell distribution determination. To determine Coumarin-6 loaded LPN incorporation into HEI-OC1, cells were also seeded in a 20 mm confocal dish for 24 h under the same conditions as previously reported and incubated together with the suspension of Coumarin-6 loaded LPNs (800 ng mL^{-1}) in a serum-free medium, and then the cells were fixed in 4% PFA at different time points (0 hour, 1 hour, 12 hours, 24 hours, and 48 hours). The samples were permeabilized with 1% Triton X-100 for half an hour and then blocked with 5% goat serum for half an hour. After washing the samples three times with PBS for five minutes each, cells were incubated with TRITC phalloidin (AAT Bioquest, 1 : 1000, 23 102) at room temperature for 1 hour, followed by three washes with PBS for five minutes each. Afterward, they were incubated with Hoechst 33342 (Solarbio, 1 : 5000, B8040) at room temperature for 30 minutes, followed by three washes with PBS. The fluorescence intensity of incorporated Coumarin-6 loaded LPNs was detected using a confocal microscope (Leica Microsystems, Germany). The excitation wavelengths for Coumarin-6 and TRITC phalloidin were 450 and 540 nm. Experiments were performed in triplicate and 3 microphotographs were obtained using the same settings for each time point.

2.2.5 LPN cell distribution in intratympanic injected C57BL/6 mice cochleae. A suspension of Coumarin-6 loaded LPNs in DMEM (Coumarin-6 concentration: 1.6 and 3.2 μg ml^{-1}) was prepared for intratympanic injection into C57BL/6 mice. Each mouse received an injection of approximately 100 μl. Cochleae were harvested at 0, 1, 12, 24 and 48 hours post-injection and fixed in 4% PFA. After 24 hours of decalcification, cochleae were dissected to isolate the apical, middle, and basal turns of the basilar membrane containing the attached organ of Corti. The dissected organs of Corti were permeabilized with 1% Triton X-100 for 30 minutes and then blocked with 5% goat serum for 30 minutes. After permeabilization and blocking, tissues were washed three times 5 minutes each in PBS on a shaker. Tissues were incubated with Phalloidin-633 (Uelandy, 1 : 500, catalog number YP0053S) at room temperature for 2 hours. Following staining, tissues were washed three times for 5 minutes each in PBS on a shaker. Next, tissues were then incubated with Hoechst 33342 (Solarbio, 1 : 5000, B8040) at room temperature for 30 minutes. Finally, tissues were washed three times for 5 minutes each in PBS. The stained organs of Corti were mounted on glass slides using 2 μl of anti-fade mounting medium (Beyotime, P0126) and cover-slipped. The samples were imaged using a confocal microscope (LSM 880) with a 633 nm channel for Phalloidin-633, a 450 nm channel for Coumarin-6 and a DAPI channel for Hoechst 33342. Experiments were performed in triplicate and three microphotographs were obtained using the same settings for each time point.

2.2.6 Auditory brainstem response (ABR) test for intratympanically injected C57BL/6 mice. Male C57BL/6 mice (8 weeks old) were obtained from Zhuhai BesTest Biotech Co., Ltd. All procedures were approved by the Experimental Animal Ethics Committee of the Guangzhou Lani Scientific Animal Center (Ethics No. G2023198). Animals were maintained under

standard husbandry conditions and anesthetized with 1% pentobarbital sodium. ABR thresholds were recorded using a BioSigRP Tucker-Davis Technology acoustic system at 4, 8, 16, and 32 kHz and were defined as the lowest stimulus intensity eliciting a reproducible wave I. Measurements were performed by two investigators blinded to group allocation.[29] Baseline body weight and ABR thresholds were obtained on day 0. Three experimental groups ($n = 10$ per group) then received a single intraperitoneal injection of cisplatin at 11, 12, or 14 mg kg^{-1} to induce sensorineural hearing loss, while five control mice received an equivalent volume of saline intraperitoneally. Body weight was monitored daily. On day 5 post-injection,[30] ABR thresholds were reassessed at the same frequencies. Considering threshold elevation and mortality, 11 mg kg^{-1} was identified as the optimal ototoxic dose, producing a stable ABR increase with a low death rate, and was therefore used to establish the mouse model. For subsequent interventions, each group ($n = 6$ per group) received an intratympanic injection of either 3.2 μg mL^{-1} raw intratympanic injection of dexamethasone or dexamethasone-loaded LPNs 2 hours before intraperitoneal administration of 11 mg per kg cisplatin. One control group ($n = 6$) received an intratympanic injection of an equivalent volume of saline. Mice were weighed daily until the next ABR assessment.

3. Results

3.1 Preparation and characterization of dexamethasone-loaded LPNs

The quality of dexamethasone-loaded LPNs was systematically evaluated through comprehensive characterization of particle size, polydispersity index (PDI), and ζ-potential. Field emission scanning electron microscopy (FESEM) combined with ImageJ software analysis demonstrated a predominant particle diameter of around 150 nm (Fig. 1A and B). Complementary characterization using laser Doppler electrophoresis (LDE) analysis revealed that the fabricated LPNs exhibited a mean particle size of approximately 380.5 nm (Table 1). The discrepancy in particle size observed between FESEM imaging and LDE analysis was likely attributable to the agglomeration of the fabricated LPNs in their colloidal state. Inter-particle interactions promoted this agglomeration, leading to an apparent increase in particle size when measured using the LDE method. The nanoscale dimension measured from FESEM imaging is particularly advantageous for biological applications, as nanoparticles below 150 nm have been shown to facilitate optimal absorption rates through clathrin-dependent and macropinocytosis-mediated endocytosis pathways, enabling efficient transport across the round window membrane and cellular uptake.[31,32]

The polydispersity index (PDI), a critical parameter reflecting the size distribution homogeneity of nanoparticles, was determined to be 0.233 for the prepared LPNs (Table 1). This value falls within the optimal range (≤0.3) for drug delivery applications, indicating a sufficiently uniform particle size distribution for effective cell targeting.[31]

The colloidal stability of the LPNs was assessed through ζ-potential measurements, which yielded a value of −21.9 mV (Table 1). While colloidal systems with ζ-potential values exceeding ± 30 mV are considered highly stable due to strong electrostatic repulsion forces that prevent particle aggregation,[33] the obtained value of ± 21.9 mV still ensures adequate stability of the LPN preparation for therapeutic applications. The slightly reduced ζ-potential further supported the likelihood of LPN agglomeration in the colloidal state, contributing to the increased particle size observed through the LDE method. These comprehensive physicochemical characterization studies collectively demonstrate that the developed dexamethasone-loaded LPNs possess optimal characteristics for potential drug delivery applications.

Fourier Transform Infrared Spectroscopy (FTIR) analysis confirmed the successful encapsulation of dexamethasone within the LPNs. The FTIR spectra revealed distinct peaks corresponding to the functional group's characteristic of dexamethasone.

Table 1 Physicochemical characteristics of dexamethasone-loaded LPNs[c]

	Particle size (nm)			
LPNs	LDE[a]	FESEM[b]	PDI	ζ potential (mV)
Dex-LPNs	380.5 ± 7.671	150	0.233 ± 0.023	−21.9 ± 0.755

[a] LDE ($n = 3$). [b] FESEM ($n = 300$). All results are expressed as mean ± SD. [c] Abbreviations: LPNs, lipid-polymer nanoparticles; Dex-LPNs, dexamethasone-loaded lipid-polymer nanoparticles; LDE, laser Doppler electrophoresis; FESEM, field emission scanning electron microscopy; *n*, number; SD, standard deviation.

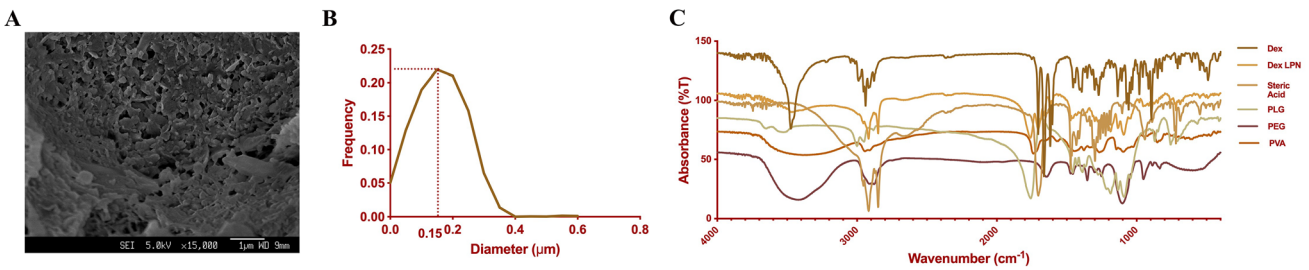

Fig. 1 Characteristics of dexamethasone-loaded LPNs. (A) Scanning electron microscopy (SEM) image of dexamethasone-loaded LPNs. (B) Particle size distribution analyzed using ImageJ. (C) High-performance liquid chromatography (HPLC) analysis to determine the drug content within the nanoparticles.

Specifically, a broad peak at 3476 cm^{-1} was observed, attributed to the stretching vibration of the hydroxyl (OH) group, providing insights into the structure of the hydroxyl groups within the molecule. Additionally, peaks at 2989 cm^{-1} were identified, corresponding to the stretching vibrations of methyl (CH_3) and methylene (CH_2) groups. The presence of a peak at 1704 cm^{-1} indicated the stretching vibrations of the carbonyl (C=O) group, associated with ketone or ester functionalities, while a peak at 1662 cm^{-1} was attributed to the stretching vibrations of the carbon–carbon double bond (C=C). These characteristic bands, which are unique to the chemical structure of dexamethasone, were also observed in the FTIR spectrum of the dexamethasone-loaded LPNs, confirming the successful encapsulation of dexamethasone within the LPNs (Fig. 1C).

3.2 *In vitro* release of dexamethasone-loaded LPNs

HPLC analysis confirmed a high dexamethasone encapsulation efficiency (EE) of 91.29 ± 0.03% and a drug loading of 14.43 ± 0.05%. The *in vitro* release profile of dexamethasone from the LPNs is illustrated in Fig. 2. Approximately 55.56% of the encapsulated dexamethasone was released within the first 4 hours, with nearly 100% release achieved over a period of 72 h. The release kinetics exhibited a biphasic pattern, characterized by an initial burst release within the first 5 h (68% release), followed by a prolonged, sustained release lasting beyond 72 h. In contrast, the control group, consisting of raw dexamethasone without encapsulation, exhibited moderately slower release after 5 h (53% release), with only 70% release after 72 hours. The encapsulation of dexamethasone within the LPNs effectively enhanced the bioavailability of hydrophobic dexamethasone by improving its release profile, highlighting the potential of LPNs as a sustained drug delivery system. This sustained release profile suggests that the LPNs can provide a prolonged therapeutic effect, which is advantageous for applications requiring long-lasting and sustained drug delivery. The *in vitro* release data demonstrated the ability of the LPNs to sustain the release of the drug over an extended period.

3.3 Effects of dexamethasone-loaded LPNs on cell proliferation

The protective effects of raw dexamethasone and dexamethasone-loaded LPNs on cisplatin-induced cytotoxicity in HEI-OC1 cells were evaluated using the Cell Counting Kit-8 (CCK-8) assay, a colorimetric method that measures cell viability based on the reduction of a tetrazolium salt to formazan dye, detectable at 450 nm. We first confirmed that neither raw dexamethasone nor dexamethasone-loaded LPNs was intrinsically cytotoxic: HEI-OC1 cells maintained 91–110% viability after 48 h of exposure to 0.8–25.6 μg mL^{-1} (Fig. 3A and B; $p > 0.05$ *vs.* untreated). In the presence of 15 μM cisplatin, dexamethasone-loaded LPNs conferred a clear, dose-dependent survival advantage over raw dexamethasone, most evident at higher concentrations (Fig. 3C). Time-course analysis at 0.8 μg mL^{-1} showed that dexamethasone-loaded LPNs became significantly superior from 48 h onward and continued to increase at 60 h (164.2 ± 3.2% *vs.* 135.9 ± 4.2%; Fig. 3D; $p < 0.001$), indicating sustained protection. Together, these findings demonstrate a dose-dependent and time-dependent enhancement of otoprotective efficacy with dexamethasone-loaded LPNs, whereas raw dexamethasone provides meaningful benefit primarily at lower concentrations.

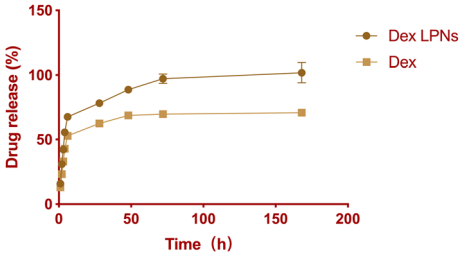

Fig. 2 *In vitro* release kinetics of dexamethasone from LPNs over a period of 168 hours. The graph illustrates rapid initial release, with approximately 55.56% of the drug being released within the first 4 hours, culminating in nearly complete release after 72 hours.

3.4 LPN distribution in cells and cochleae

To investigate the *in vitro* and *in vivo* distribution and metabolic dynamics of LPNs, we employed confocal microscopy to track the fluorescence metabolism of LPNs in HEI-OC1 cells and the cochlear organ of Corti at various time points, followed by quantitative analysis. Coumarin-6 labeled LPNs were efficiently taken up by HEI-OC1 cells, with fluorescence intensity within the cells increasing significantly over a 48-hour period ($P < 0.001$). The granular green fluorescence, localized widely in the cytoplasm, showed a gradual increase throughout the observation period, confirming enhanced cellular uptake of the LPNs over time (Fig. 4). *In vivo*, the results demonstrated that the LPNs did not cause damage to hair cells. Coumarin-6-labeled LPNs (3.2 μg mL^{-1}) were readily visualized by confocal microscopy. The strongest fluorescence intensity was observed in the basal turn of the cochlea, suggesting a higher concentration or metabolic activity of nanoparticles in this region. Over time, the fluorescence intensity increased, peaking at 24 hours, where it was approximately twice the intensity observed at the 0-hour mark. This increase is likely attributed to the accumulation or metabolic processing of nanoparticles within the cochlea. Subsequently, the fluorescence intensity began to decline, potentially due to the metabolic excretion or degradation of the nanoparticles (Fig. 5, $P < 0.01$ and $P < 0.001$). These findings provide valuable insights into the spatial and temporal distribution of LPNs within cells and cochlear tissues and are critical for understanding the kinetics and efficiency of LPN-based drug delivery systems.

3.5 Effects of dexamethasone-loaded LPNs on ABR

Mice were assigned to four groups: a physiological saline control group and three cisplatin groups receiving 11, 12, or 14 mg kg^{-1} intraperitoneally. The observed mortality rates were 0% (11 mg kg^{-1}), 60% (12 mg kg^{-1}), and 80% (14 mg kg^{-1}). Surviving animals (10, 4, and 2 mice, respectively) underwent ABR testing to evaluate cochlear function. As shown in Fig. 6A,

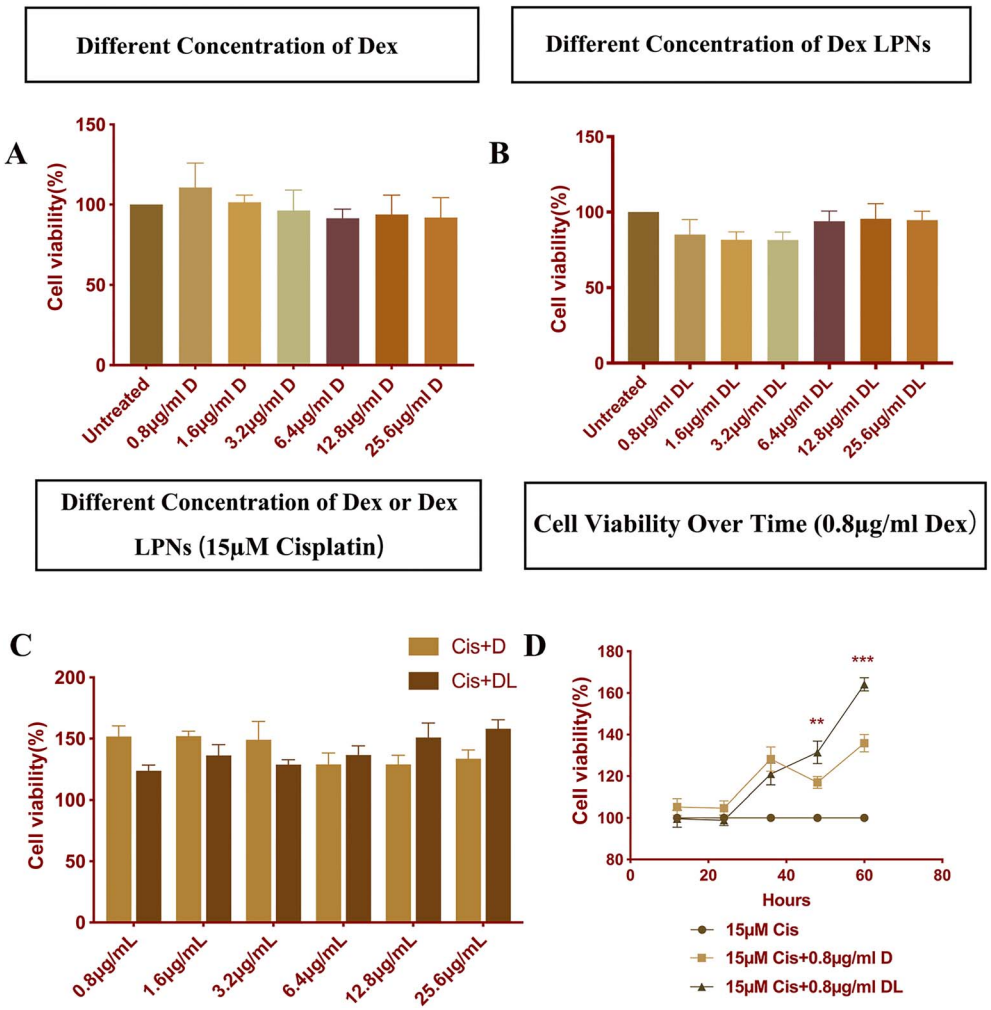

Fig. 3 Protective effects of dexamethasone formulations on cisplatin-induced cytotoxicity in HEI-OC1 cells assessed by CCK-8 assay. (A) Cell viability after 48 h of exposure to increasing concentrations of raw Dex (0.8–25.6 μg ml^{-1}). (B) Cell viability after 48 h of exposure to Dex-LPNs at matched Dex concentrations. (C) Viability of cells co-treated with 15 μM Cis and raw Dex or Dex-LPNs for 48 h. (D) Time-course of cell viability under 15 μM Cis with 0.8 μg ml per ml Dex or Dex-LPNs over 12–60 h (**$p < 0.01$ and ***$p < 0.001$ *vs.* Cis alone). Data are presented as mean ± SD ($n = 3$). *$p < 0.05$, **$p < 0.01$, and ***$p < 0.001$.

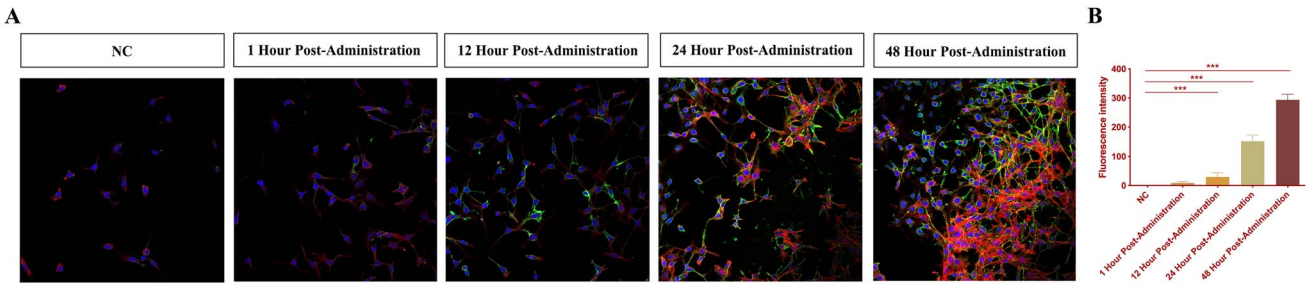

Fig. 4 *In vitro* metabolism of LPNs in HEI-OC1 cells. (A) Confocal microscopy images show the uptake of Coumarin-6-labeled LPNs in HEI-OC1 cells over 1, 12, and 24 hours. Phalloidin (red) labels the cytoskeleton, DAPI (blue) labels the cell nucleus, and green fluorescence represents the excitation light of the LPNs. (B) Fluorescence intensity was quantified using ImageJ to evaluate LPN uptake. The excitation light was observed as granular signals within the cytoplasm, with intensity gradually increasing over time. ***P <0.001.

ABR thresholds normalized to the physiological saline control increased in a dose-dependent manner after cisplatin administration, indicating progressive ototoxicity. Based on combined analysis of ABR thresholds and mortality, 11 mg kg^{-1} was selected as the optimal dose for subsequent experiments. For the treatment study, one control group received intratympanic

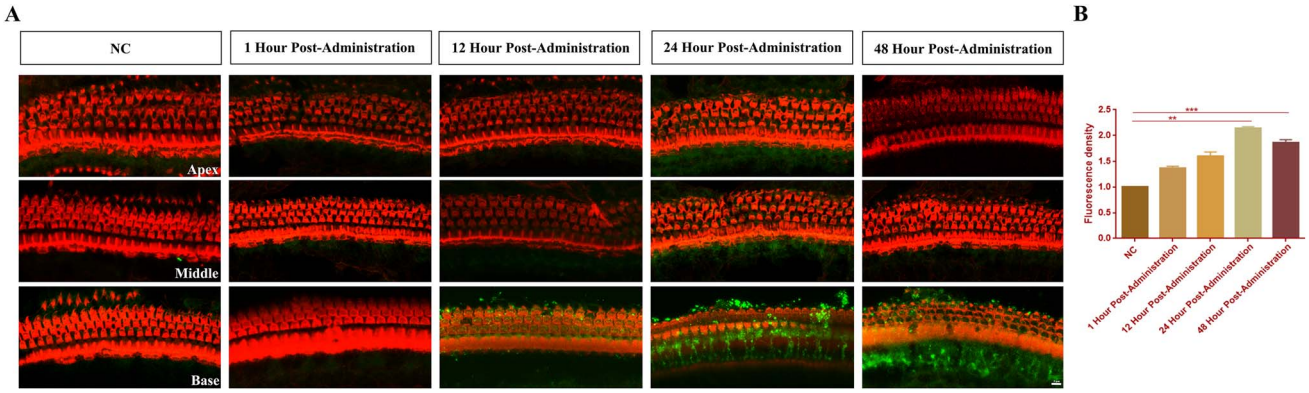

Fig. 5 *In vivo* metabolism of LPNs within the cochlea. (A) Fluorescence metabolism of nanoparticles at various time points. (B) Quantitative analysis of LPN distribution in the organs of Corti. Phalloidin (red) labels the hair cells, while green fluorescence represents the excitation light of the LPNs. The results demonstrate that LPNs do not cause damage to hair cells. The strongest fluorescence intensity is observed at the basal turn, gradually increasing over time. At 24 hours, the fluorescence intensity peaks at approximately twice the level observed at the 0-hour mark, after which it begins to decline. Scale bar: 5 μm. $^{**}P < 0.01$ and $^{***}P < 0.001$.

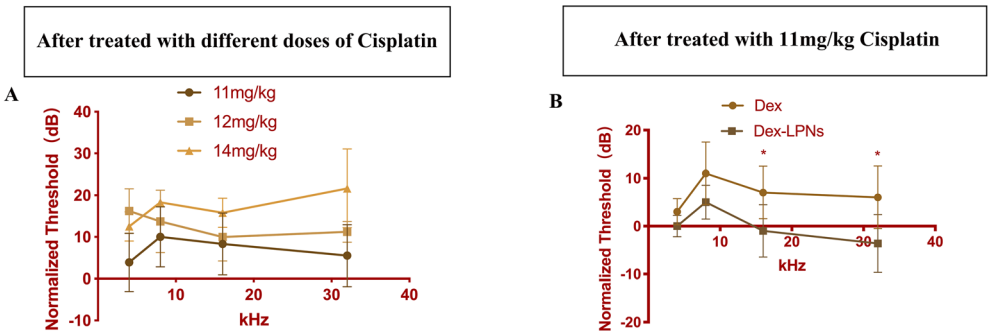

Fig. 6 (A) Establishment and optimization of the cisplatin-induced ototoxicity model. A mouse model for cisplatin-induced ototoxicity using varying doses of cisplatin (11 mg kg^{-1}, 12 mg kg^{-1}, and 14 mg kg^{-1}) was established. Day-5 mortality and subsequent evaluation of ABR threshold shifts (normalized to saline controls) increased in a dose-dependent manner, identifying 11 mg kg^{-1} as the optimal dose for subsequent experiments. (B) Therapeutic efficacy of raw dexamethasone and dexamethasone loaded LPNs in the cisplatin-induced ototoxicity model. Intratympanic injection of 3.2 μg per ml dexamethasone-loaded LPNs showed lower ABR thresholds across all tested frequencies compared with raw dexamethasone, with significant differences at 16 and 32 kHz. $^{*}P < 0.05$.

physiological saline. Two experimental groups received intratympanic injections of either 3.2 μg per mL dexamethasone-loaded LPNs or raw dexamethasone, and two hours later, 11 mg per kg cisplatin was administered intraperitoneally. Five days thereafter, ABR thresholds normalized to the control were consistently lower at all tested frequencies in the dexamethasone-loaded LPNs group than in the raw dexamethasone group, with significant differences at 16 and 32 kHz (Fig. 6B). These results indicate that dexamethasone-loaded LPNs provide superior protection against cisplatin-induced ototoxicity, potentially through enhanced delivery and sustained release within the cochlear environment.

4. Discussion

This work presents a hybrid delivery system that integrates a stearic-acid lipid monolayer, a PLGA core, and a PEG-400 shell to combine high biocompatibility, improved payload, sustained release, and *in vivo* efficacy. The stearic-acid interface enhances encapsulation of hydrophobic dexamethasone, while PLGA mitigates the instability, lipid peroxidation, and burst release commonly seen with conventional lipid carriers.[13,33] PEG-400 reduces opsonization and prolongs circulation.[16,34] Consistent with these design goals, the ζ-potential (−21.9 mV) falls within the typical range for stearic-acid surfaces (−20 to −30 mV), supporting colloidal stability, and the narrow size distribution (PDI = 0.23) indicates uniformity favorable for reproducible loading and release.[32,35] This multi-layered design is critical for achieving successful targeted delivery. Supporting this, Gu J. *et al.* previously reported that lipid (DMPC)-polymer (mPEG-PLA) hybrid nanoparticle loaded astaxanthin enabled this poorly soluble drug to possess favorable biocompatibility and penetrate the round window membrane.[30] Accordingly, the biphasic release profile—an early local burst followed by prolonged release—likely enhances therapeutic performance by rapidly establishing and then maintaining effective dexamethasone exposure at cochlear targets.

At the cellular level, CCK-8 assays confirmed the absence of intrinsic cytotoxicity, and fluorescence imaging demonstrated progressive intracellular accumulation in HEI-OC1 cells (1–48 h), whereas *in vivo* cochlear fluorescence peaked at around 24 h and declined by 48 h (Fig. 4 and 5). The divergence likely reflects proliferative cell culture *versus* non-dividing cochlear hair cells with active clearance. These observations are broadly concordant with previous kinetics studies of the cochlea[35,36] and suggest higher cochlear accumulation compared with certain formulations and the administration route reported by Sun *et al.*[37]

Functionally, cisplatin produced dose-dependent ABR threshold shifts and mortality across 11–14 mg kg^{-1} (Fig. 6A); 11 mg kg^{-1} was selected as the optimal ototoxic dose because it balanced robust threshold elevation with acceptable mortality. Against this background, dexamethasone-loaded LPNs outperformed raw dexamethasone in attenuating hearing loss, yielding lower baseline-normalized ABR thresholds across tested frequencies, with significant advantages at 16 and 32 kHz. This pattern is consistent with improved intracochlear exposure (*e.g.*, more efficient round-window permeation) and sustained release that may prolong therapeutic level relative to raw dexamethasone's transient peak during the cisplatin injury window. Furthermore, because ABR threshold elevations correlated closely with outer-hair-cell loss, the observed functional protection plausibly reflects reduced hair-cell injury,[38,39] although confirmation will require cochlear histopathology in future work.

Mechanistically, cisplatin traverses the blood-labyrinth barrier, preferentially accumulates in the stria vascularis, and persists long-term, thereby disrupting endolymphatic homeostasis and triggering inflammatory responses in outer hair cells.[40,41] Dexamethasone mitigates these effects primarily through glucocorticoid receptor-mediated suppression of pro-inflammatory signaling (*e.g.*, TNF-α, IL-6, and NF-κB) and by preserving cochlear microvascular perfusion.[42] Consequently, formulations that sustain intracochlear residence and maintain pharmacologically active exposure are expected to provide more durable protection against cisplatin's prolonged cochlear burden.[43] The sustained-release kinetics of our hybrid LPNs meet these requirements, likely explaining their superior functional performance. Nevertheless, direct evaluation of inner-ear pharmacokinetics and pharmacodynamics is essential to substantiate this interpretation. Collectively, these findings support nanoparticles as viable cochlear carriers and highlight the need to account for cochlear metabolic behavior when optimizing composition, dose, and exposure duration to sustain intralabyrinthine concentrations while minimizing adverse effects.

5. Conclusion

This study provides valuable insights into the encapsulation efficiency, cellular uptake, and therapeutic outcomes of dexamethasone-loaded LPNs. By examining the drug delivery efficiency in both cellular and animal models, the study aims to establish a foundation for the potential clinical application of LPNs in enhancing the treatment of SNHL, particularly in the context of ototoxicity induced by chemotherapeutic agents. This research contributes to the ongoing efforts to improve the management of SNHL, offering a novel approach that may lead to more effective treatments and better patient outcomes.

Conflicts of interest

There are no conflicts to declare.

Data availability

All data supporting the findings of this study are available within the article. Additional raw data can be provided by the corresponding author upon reasonable request.

Acknowledgements

This work was supported by the Guangzhou Municipal Basic and Applied Basic Research Program (Grant No. 202201011557), funded by the Guangzhou Municipal Science and Technology Bureau.

References

1 A. Chattaraj, M. P. Syed, C. A. Low and T. K. Owonikoko, Cisplatin-Induced Ototoxicity: A Concise Review of the Burden, Prevention, and Interception Strategies, *JCO Oncol. Pract.*, 2023, **19**(5), 278–283, DOI: **10.1200/OP.22.00710**.

2 V. A. Sanchez, M. M. Shuey, P. C. Dinh Jr, P. O. Monahan, S. D. Fosså, H. D. Sesso, M. E. Dolan, L. H. Einhorn, D. J. Vaughn, N. E. Martin, D. R. Feldman, K. Kroenke, C. Fung, R. D. Frisina and L. B. Travis, Patient-Reported Functional Impairment Due to Hearing Loss and Tinnitus After Cisplatin-Based Chemotherapy, *J. Clin. Oncol.*, 2023, **41**(12), 2211–2226, DOI: **10.1200/JCO.22.01456**.

3 L. K. Dillard, L. Lopez-Perez, R. X. Martinez, A. M. Fullerton, S. Chadha and C. M. McMahon, Global burden of ototoxic hearing loss associated with platinum-based cancer treatment: A systematic review and meta-analysis, *Cancer Epidemiol.*, 2022, **79**, 102203, DOI: **10.1016/j.canep.2022.102203**.

4 T. Marshak, M. Steiner, M. Kaminer, L. Levy and A. Shupak, Prevention of Cisplatin-Induced Hearing Loss by Intratympanic Dexamethasone: A Randomized Controlled Study, *Otolaryngol., Head Neck Surg.*, 2014, **150**(6), 983–990, DOI: **10.1177/0194599814524894**.

5 Q. Qiang, X. Wu, T. Yang, C. Yang and H. Sun, A comparison between systemic and intratympanic steroid therapies as initial therapy for idiopathic sudden sensorineural hearing loss: a meta-analysis, *Acta Otolaryngol.*, 2017, **137**(6), 598–605, DOI: **10.1080/00016489.2016.1260157**.

6 H. Li, G. Feng, H. Wang and Y. Feng, Intratympanic steroid therapy as a salvage treatment for sudden sensorineural hearing loss after failure of conventional therapy: a meta-analysis of randomized, controlled trials, *Clin. Ther.*, 2015, **37**(1), 178–187, DOI: **10.1016/j.clinthera.2014.11.009**.

7 M. E. Smith, R. Knappett, D. Vickers, D. White, C. J. Schramm, S. Mehta, Y. Sun, B. Watkins, M. Chadburn, H. Jarrett, K. James, E. Brettell, T. E. Roberts, M. L. Bance and J. R. Tysome, Protocol for a multicentre randomised controlled trial of STeroid Administration Routes For Idiopathic Sudden sensorineural Hearing loss: The STARFISH trial, *PLoS One*, 2024, **19**(2), e0290480, DOI: **10.1371/journal.pone.0290480**.

8 M. Oray, K. Abu Samra, N. Ebrahimiadib, H. Meese and C. S. Foster, Long-term side effects of glucocorticoids, *Expet Opin. Drug Saf.*, 2016, **15**(4), 457–465, DOI: **10.1517/14740338.2016.1140743**.

9 R. M. Stanbury and E. M. Graham, Systemic corticosteroid therapy-side effects and their management, *Br. J. Ophthalmol.*, 1998, **82**(6), 704–708, DOI: **10.1136/bjo.82.6.704**.

10 R. S. Lester, S. R. Knowles and N. H. Shear, The risks of systemic corticosteroid use, *Dermatol. Clin.*, 1998, **16**(2), 277–288, DOI: **10.1016/s0733-8635(05)70010-3**.

11 Y. Zhang, H. Su, L. Wen, F. Yang and G. Chen, Mathematical modeling for local trans-round window membrane drug transport in the inner ear, *Drug Deliv.*, 2016, **23**(8), 3082–3087, DOI: **10.3109/10717544.2016.1149745**.

12 J. Hao and S. K. Li, Inner ear drug delivery: Recent advances, challenges, and perspective, *Eur. J. Pharm. Sci.*, 2019, **126**, 82–92, DOI: **10.1016/j.ejps.2018.05.020**.

13 Š. Kordiš, D. Vozel, M. Hribar, N. B. Urbančič and S. Battelino, The Outcome of Prompt Concomitant Single-Dose High-Concentration Intratympanic and Tapered Low-Dose Oral Systemic Corticosteroid Treatment for Sudden Deafness, *J. Int. Adv. Otol.*, 2020, **16**(2), 201–206, DOI: **10.5152/iao.2020.8341**.

14 N. J. Creber, H. T. Eastwood, A. J. Hampson, J. Tan and S. J. O'Leary, Adjuvant agents enhance round window membrane permeability to dexamethasone and modulate basal to apical cochlear gradients, *Eur. J. Pharm. Sci.*, 2019, **126**, 69–81, DOI: **10.1016/j.ejps.2018.08.013**.

15 D. H. Kim, T. N. Nguyen, Y. M. Han, P. Tran, J. Rho, J. Y. Lee, H. Y. Son and J. S. Park, Local drug delivery using poly (lactic-co-glycolic acid) nanoparticles in thermosensitive gels for inner ear disease treatment, *Drug Deliv.*, 2021, **28**(1), 2268–2277, DOI: **10.1080/10717544.2021.1992041**.

16 E. Lehner, A. Liebau, F. Syrowatka, W. Knolle, S. K. Plontke and K. Mäder, Novel biodegradable Round Window Disks for inner ear delivery of dexamethasone, *Int. J. Pharm.*, 2021, **594**, 120180, DOI: **10.1016/j.ijpharm.2020.120180**.

17 R. Tenchov, R. Bird, A. E. Curtze and Q. Zhou, Lipid Nanoparticles-From Liposomes to mRNA Vaccine Delivery, a Landscape of Research Diversity and Advancement, *ACS Nano*, 2021, **15**(11), 16982–17015, DOI: **10.1021/acsnano.1c04996**.

18 Y. He, Z. Chen, Q. Liu, Z. Li, D. Wen, H. Zhang, M. Zhang, D. Jiang, H. Li, L. Wen and G. Chen, Reversible opening of the blood-labyrinth barrier by low-pressure pulsed ultrasound and microbubbles for the treatment of inner ear diseases, *J. Contr. Release*, 2024, **372**, 318–330, DOI: **10.1016/j.jconrel.2024.06.043**.

19 A. Movahedpour, R. Taghvaeefar, A. A. Asadi-Pooya, Y. Karami, R. Tavasolian, S. H. Khatami, E. Soltani Fard, S. Taghvimi, N. Karami, K. Rahimi Jaberi, M. Taheri-Anganeh and H. Ghasemi, Nano-delivery systems as a promising therapeutic potential for epilepsy: Current status and future perspectives, *CNS Neurosci. Ther.*, 2023, **29**(11), 3150–3159, DOI: **10.1111/cns.14355**.

20 N. K. Dastgerdi, N. K. Dastgerdi, H. Bayraktutan, G. Costabile, F. Atyabi, R. Dinarvand, G. Longobardi, C. Alexander and C. Conte, Enhancing siRNA cancer therapy: Multifaceted strategies with lipid and polymer-based carrier systems, *Int. J. Pharm.*, 2024, **663**, 124545, DOI: **10.1016/j.ijpharm.2024.124545**.

21 H. Tonbul, A. Şahin, S. C. Öztürk, G. Ultav, E. Tavukçuoğlu, S. Akbaş, Y. Aktaş, G. Esendağlı and Y. Çapan, An all-in-one nanoparticle for overcoming drug resistance: doxorubicin and elacridar co-loaded folate receptor targeted PLGA/MSN hybrid nanoparticles, *J. Drug Target.*, 2024, **5**, 1–10, DOI: **10.1080/1061186X.2024.2374034**.

22 C. Pereira-Leite, M. Bom, A. Ribeiro, C. Almeida and C. Rosado, Exploring Stearic-Acid-Based Nanoparticles for Skin Applications—Focusing on Stability and Cosmetic Benefits, *Cosmetics*, 2023, **10**, 99.

23 B. Mandal, H. Bhattacharjee, N. Mittal, H. Sah, P. Balabathula, L. A. Thoma and G. C. Wood, Core-shell-type lipid-polymer hybrid nanoparticles as a drug delivery platform, *Nanomedicine*, 2013, **9**, 474–491.

24 X. An, C. Zhong, B. Han, E. Chen, Q. Zhu, Y. Yang, R. Li, R. Yang, D. Zha and Y. Han, Lysophosphatidic acid exerts protective effects on HEI-OC1 cells against cytotoxicity of cisplatin by decreasing apoptosis, excessive autophagy, and accumulation of ROS, *Cell Death Discov.*, 2023, **9**(1), 415, DOI: **10.1038/s41420-023-01706-5**.

25 V. A. Sanchez, P. C. Dinh Jr, P. O. Monahan, S. Althouse, J. Rooker, H. D. Sesso, M. E. Dolan, M. Weinzerl, D. R. Feldman, C. Fung, L. H. Einhorn, R. D. Frisina and L. B. Travis, Comprehensive Audiologic Analyses After Cisplatin-Based Chemotherapy, *JAMA Oncol.*, 2024, **10**(7), 912–922, DOI: **10.1001/jamaoncol.2024.1233**.

26 M. Iqbal, N. Zafar, H. Fessi and A. Elaissari, Double emulsion solvent evaporation techniques used for drug encapsulation, *Int. J. Pharm.*, 2015, **496**(2), 173–190, DOI: **10.1016/j.ijpharm.2015.10.057**.

27 G. M. Kalinec, C. Park, P. Thein and F. Kalinec, Working with Auditory HEI-OC1 Cells, *J. Vis. Exp.*, 2016, (115), 54425, DOI: **10.3791/54425**.

28 M. Nie, G. Chen, C. Zhao, J. Gan, M. Alip, Y. Zhao and L. Sun, Bio-inspired adhesive porous particles with human MSCs encapsulation for systemic lupus erythematosus treatment, *Bioact. Mater.*, 2020, **6**(1), 84–90, DOI: **10.1016/j.bioactmat.2020.07.018**.

29 F. Wu, H. Xiong and S. Sha, Noise-induced loss of sensory hair cells is mediated by ROS/AMPKα pathway, *Redox Biol.*, 2020, **29**, 101406, DOI: **10.1016/j.redox.2019.101406**.

30 J. Gu, Y. Chen, L. Tong, X. Wang, D. Yu and H. Wu, Astaxanthin-loaded polymer-lipid hybrid nanoparticles (ATX-LPN): assessment of potential otoprotective effects, *J.*

Nanobiotechnol., 2020, **18**(1), 53, DOI: **10.1186/s12951-020-00600-x**, IF: 10.6 Q1. Erratum in: *J. Nanobiotechnology*, 2020 May 19, **18**, (1), 78, 10.1186/s12951-020-00627-0IF: 10.6 Q1, PMID: 32192504IF: 10.6 Q1; PMCID: PMC7081530IF: 10.6 Q1.

31 M. Danaei, M. Dehghankhold, S. Ataei, F. Hasanzadeh Davarani, R. Javanmard, A. Dokhani, S. Khorasani and M. R. Mozafari, Impact of Particle Size and Polydispersity Index on the Clinical Applications of Lipidic Nanocarrier Systems, *Pharmaceutics*, 2018, **10**(2), 57, DOI: **10.3390/pharmaceutics10020057**.

32 M. V. Goycoolea and L. Lundman, Round window membrane. Structure function and permeability: a review, *Microsc. Res. Tech.*, 1997, **36**(3), 201–211, DOI: **10.1002/(SICI)1097-0029(19970201)36:3<201::AID-JEMT8>3.0.CO;2-R**.

33 R. Shah, D. Eldridge, E. Palombo and I. Harding, Optimisation and Stability Assessment of Solid Lipid Nanoparticles using Particle Size and Zeta Potential, *J. Phys. Sci.*, 2014, **25**(1), 59–75.

34 A. Mohanty, S. Uthaman and I. K. Park, Utilization of Polymer-Lipid Hybrid Nanoparticles for Targeted Anti-Cancer Therapy, *Molecules*, 2020, **25**(19), 4377, DOI: **10.3390/molecules25194377**.

35 R. M. Shah, D. Rajasekaran, M. Ludford-Menting, D. S. Eldridge, E. A. Palombo and I. H. Harding, Transport of stearic acid-based solid lipid nanoparticles (SLNs) into human epithelial cells, *Colloids Surf., B*, 2016, **140**, 204–212, DOI: **10.1016/j.colsurfb.2015.12.029**.

36 R. Martin-Saldana, A. Palao-Suay, M. R. Trinidad, M. R. Aguilar, R. Ramirez-Camacho and J. San Roman, Otoprotective properties of 6alpha-methylprednisolone-loaded nanoparticles against cisplatin: *In vitro* and *in vivo* correlation, *Nanomed. Nanotechnol. Biol. Med.*, 2016, **12**(4), 965–976, DOI: **10.1016/j.nano.2016.02.009**.

37 C. Sun, X. Wang, D. Chen, X. Lin, D. Yu and H. Wu, Dexamethasone loaded nanoparticles exert protective effects against cisplatin-induced hearing loss by systemic administration, *Neurosci. Lett.*, 2016, **619**, 142–148, DOI: **10.1016/j.neulet.2016.05.042**.

38 A. Ekborn, G. Laurell, H. Ehrsson and J. Miller, Intracochlear administration of thiourea protects against cisplatin-induced outer hair cell loss in the guinea pig, *Hear Res*, 2003, **181**(1–2), 109–115, DOI: **10.1016/s0378-5955(03)00181-3**.

39 R. P. Hamernik and W. Qiu, Correlations among evoked potential thresholds, distortion product otoacoustic emissions and hair cell loss following various noise exposures in the chinchilla, *Hear Res*, 2000, **150**(1–2), 245–257, DOI: **10.1016/s0378-5955(00)00204-5**.

40 A. M. Breglio, A. E. Rusheen, E. D. Shide, K. A. Fernandez, K. K. Spielbauer, K. M. McLachlin, M. D. Hall, L. Amable and L. L. Cunningham, Cisplatin is retained in the cochlea indefinitely following chemotherapy, *Nat. Commun.*, 2017, **8**(1), 1654, DOI: **10.1038/s41467-017-01837-1**.

41 M. A. Ingersoll, R. D. Lutze, C. K. Pushpan, R. G. Kelmann, H. Liu, M. T. May, W. J. Hunter, D. Z. He and T. Teitz, Dabrafenib protects from cisplatin-induced hearing loss in a clinically relevant mouse model, *JCI Insight*, 2023, **8**(24), e171140, DOI: **10.1172/jci.insight.171140**.

42 X. Wang, Y. Zhou, D. Wang, Y. Wang, Z. Zhou, X. Ma, X. Liu and Y. Dong, Cisplatin-induced ototoxicity: From signaling network to therapeutic targets, *Biomed. Pharmacother.*, 2023, **157**, 114045, DOI: **10.1016/j.biopha.2022.114045**.

43 M. Magdy, E. Elmowafy, M. Elassal and R. A. H. Ishak, Localized drug delivery to the middle ear: Recent advances and perspectives for the treatment of middle and inner ear diseases, *J. Drug Deliv. Sci. Technol.*, 2022, **69**, 103149, DOI: **10.1016/j.jddst.2022.103149**.

